scientific reports

Check for updates

OPEN

YTHDC1 negatively regulates UBE3A to influence RAD51 ubiquitination and inhibit apoptosis in colorectal cancer cells

Mingwei Gao[1], Yueguang Wu[1], Li Zhang[1], Yan Zhou[2], Huijuan Liu[2], Weimin Zhang[1,2], Shubin Wang[1]✉ & Yongping Cui[1,2]✉

YTHDC1, a key protein in the m^{6}A-related regulatory network within cells, is involved in multiple cellular processes such as chromatin-related regulation, RNA splicing, and nuclear export. Understanding its role in colorectal cancer (CRC) development and DNA damage repair is critical for the advancement of treatment strategies. Our study found that YTHDC1 was highly expressed in high-malignancy CRC tissues compared with low-malignancy ones. Upon silencing YTHDC1, we observed a pronounced suppression of the proliferation of CRC cell lines, accompanied by a substantial increase in cell apoptosis. Furthermore, we identified RAD51 as a crucial downstream target of YTHDC1. Knocking down YTHDC1 led to a notable decrease in RAD51 protein levels, and silencing RAD51 also inhibited cancer cell proliferation. Interestingly, RNA-sequencing data indicated that the YTHDC1 deletion did not affect RAD51 transcription. However, Western blot revealed that this deletion increased the ubiquitination of RAD51, likely due to the upregulated E3 ligase UBE3A. Ubiquitination experiments subsequently confirmed that RAD51 is indeed one of the substrates of UBE3A. In summary, our study provides novel insights into how YTHDC1 modulates the expression of RAD51 through post-translational modifications. These findings offer valuable information that may potentially contribute to the development of more effective therapeutic strategies for CRC.

Keywords YTHDC1, Colorectal tumor, RAD51, UBE3A, Cell apoptosis

N^6-methyladenosine (m^{6}A) modification is one of the most important epigenetic modifications of RNA[1,2]. Structural research has shown that YTH domain-containing proteins are vital m^{6}A readers[3,4]. These proteins exert multiple biological functions by precisely recognizing and binding to m^{6}A modification on RNA. YTHDC1, a member of the YTH family, exhibits distinct features compared to other family members such as YTHDF1/2/3 and YTHDC2. Localized in the cell nucleus, YTHDC1 has been reported to participate in chromatin-associated regulation[5,6], RNA splicing modulation[7], and nuclear-cytoplasmic transport[8]. Moreover, it is also linked to DNA replication and DNA damage repair mechanisms[9–11]. In contrast to YTHDF1/2/3, which have been extensively explored in the context of tumor research, YTHDC1 has received relatively less attention in tumor-related studies[12]. YTHDC1 has been shown to regulate gene expression by influencing the transcriptional stability of genes and facilitating the nuclear localization of circular RNA. These regulatory effects impact processes such as acute myeloid leukemia (AML) cell proliferation, neuronal viability, and the initiation and progression of colorectal cancer (CRC)[9,13–15]. Collectively, these investigations indicate that YTHDC1 is indispensable for tumorigenesis and tumor development, and its regulatory mechanisms are both diverse and intricate.

Homologous recombination (HR) repair is a highly precise DNA repair mechanism that plays a crucial role in DNA damage response and replication. RAD51, one of the key recombinases involved in this process, plays a central and indispensable role[16,17]. Emerging evidence has demonstrated that m^{6}A modification and YTHDC1 have significant implications in DNA damage repair, particularly in the homologous recombination repair pathway[11,18,19]. For instance, YTHDC1 safeguards transcribed RNA by forming DNA-RNA hybrids upon its recruitment to UV-induced DNA damage sites[10]. Additionally, studies have shown that in breast cancer cells, the

[1]Cancer Institute, Shenzhen Peking University-Hong Kong University of Science and Technology (PKU-HKUST) Medical Center, Shenzhen Key Laboratory of Gastrointestinal Cancer Translational Research, Department of Oncology, Peking University Shenzhen Hospital, Shenzhen, Guangdong, China. [2]Key Laboratory of Cellular Physiology of the Ministry of Education, Department of Pathology, Shanxi Medical University, Taiyuan, Shanxi, China. ✉email: wangshubin2013@163.com; cuiyp@sphmc.org

epidermal growth factor (EGF) transcript undergoes m^{6}A modification catalyzed by METTL3. Subsequently, YTHDC1 recognizes and binds to the m^{6}A-modified EGF transcript, leading to enhanced EGF and RAD51 expression, ultimately augmenting the efficiency of homologous recombination[11]. However, the specific regulatory mechanisms by which YTHDC1 exerts its effects in this process remain incompletely understood.

In this study, we found that high expression levels of YTHDC1 were positively correlated with poor overall survival outcomes in patients with colorectal cancer. Knockdown of YTHDC1 markedly inhibited the proliferation of colorectal cancer cells by accelerating the process of apoptosis. We identified the homologous recombinase RAD51 as a downstream target regulated by YTHDC1. Depletion of RAD51 led to a similar cellular phenotype. More importantly, we found that YTHDC1 negatively regulates the E3 ubiquitin-protein ligase UBE3A. This negative regulation results in increased ubiquitination of RAD51, which in turn promotes apoptosis in colorectal cancer cells.

Results

YTHDC1 functions as a pro-oncogenic factor in colorectal cancer

Initially, through the analysis of the TCGA (The Cancer Genome Atlas) database, we observed that patients with high YTHDC1 expression exhibited a lower overall survival (OS) rate compared to those with low expression. This tendency was also prominently evident in the relapse-free survival (RFS) rate (Fig. 1a). These findings imply that elevated YTHDC1 expression may be detrimental to patient prognosis. We conducted immunohistochemical assays on tissue microarrays obtained from 80 colorectal cancer patients (Supplementary Table S1). The results demonstrated that the number of tumor tissue sections with a YTHDC1-positive proportion exceeding 50% was significantly greater than that of adjacent tissue sections (Fig. 1b). This finding indicates that YTHDC1 is expressed at markedly higher levels in high-malignancy tissues than in low-malignancy ones. Moreover, by comparing YTHDC1 staining patterns between cancerous and normal tissue sections, we found that infiltrating tumor tissue contained a larger number of strongly YTHDC1-positive cells. In contrast, the adjacent normal colon tissue displayed lighter YTHDC1 staining and a more uniform distribution within the colon tissue (Fig. 1c). Collectively, the data suggests that YTHDC1 may serve as an oncogenic factor in colorectal cancer.

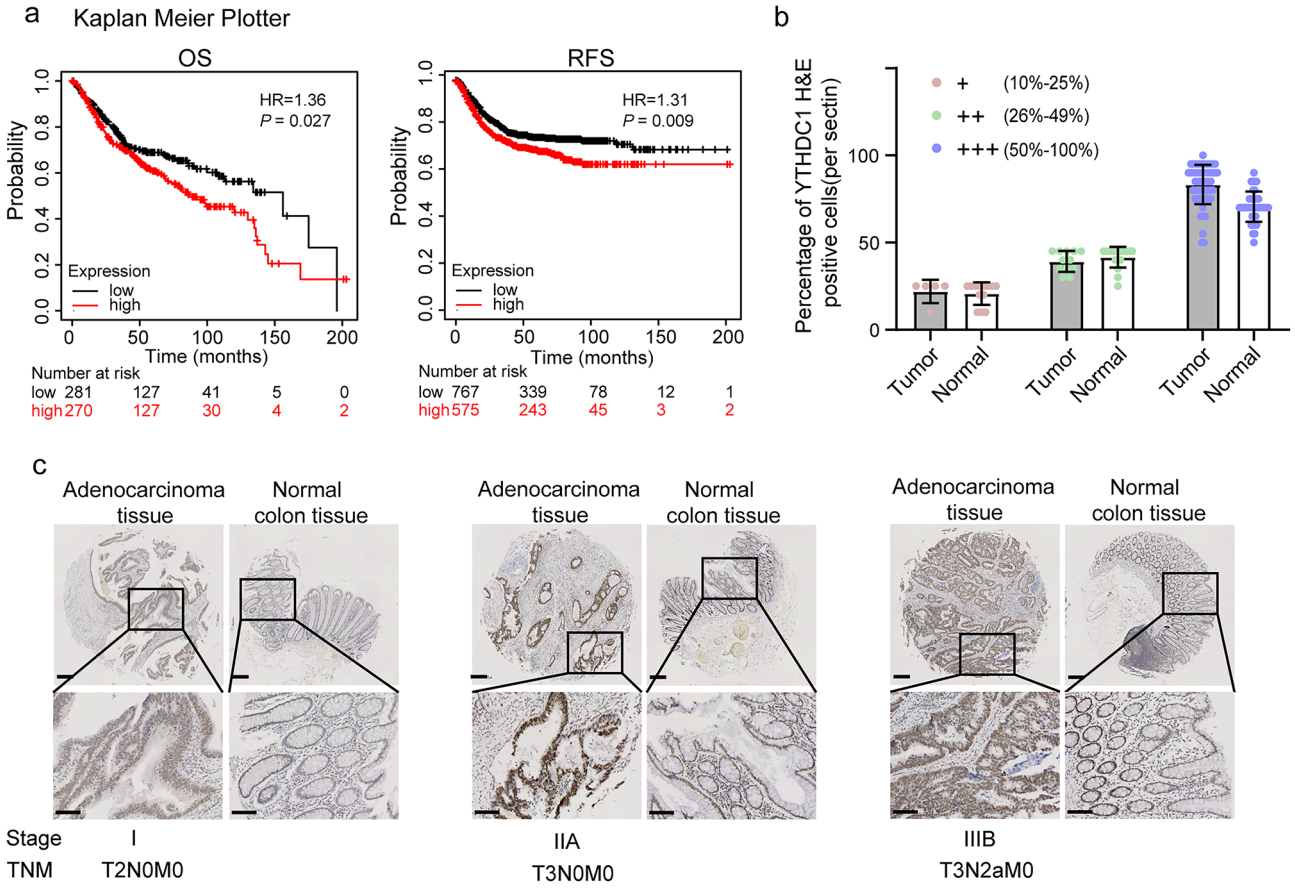

Fig. 1. YTHDC1 functions as a pro-oncogenic factor in colorectal cancer. (**a**) The association of YTHDC1 with the Overall Survival (OS) curve and Relapse-Free Survival (RFS) curve about colorectal cancer was analyzed on the Kaplan Meier plotter website. (**b**) The statistics of the percentage of YTHDC1 H&E positive cells in each section. Each dot represents a section. The quantification is from the IHC staining of 80 paired tissues. (**c**) Representative HE staining images of YTHDC1 in colorectal cancer patient tissue are presented. The scale bars are 200 μm for the upper panel and 100 μm for the lower panel (the zoomed-in images).

The deficiency of YTHDC1 suppresses the proliferation of colorectal cancer cells and increases apoptosis

To elucidate the role of YTHDC1 in colorectal cancer, we employed small interfering RNAs (siRNAs) to knockdown YTHDC1 in two distinct colorectal cancer cell lines, HCT116 and SW480 in vitro. Using Cell Counting Kit-8 (CCK8) assays, we monitored cell proliferation after YTHDC1 knockdown. The results indicated that YTHDC1 knockdown significantly inhibited the growth of both cell lines (Fig. 2a). Western blot experiments were conducted to confirm the knockdown efficiency of the two siRNAs, which exceeded 70% (Fig. 2b). Moreover, we carried out a single-cell colony formation assay, which further verified that the deficiency of YTHDC1 in HCT116 and SW480 cells significantly impeded the formation of single-cell clones (Fig. 2c, d). Given that YTHDC1 is an m^6A-binding protein, mutations at two binding sites in YTHDC1, namely W377A and W428A, lead to the loss of its binding ability[4]. To determine whether YTHDC1 inhibits the proliferation of colorectal cancer cells in an m^6A-binding dependent manner, we performed rescue experiments on YTHDC1-siRNA treated cells using WT-YTHDC1, W377A-YTHDC1, and W428A-YTHDC1 (Fig. 2e and Supplementary Fig. 1a). The results demonstrated that although the YTHDC1 mutants could marginally rescue the cell number, neither W377A-YTHDC1 nor W428A-YTHDC1 could restore the cell number to the level achieved by WT-YTHDC1. Multiple studies have shown that knockout or knockdown of METTL3 suppresses the proliferation of colorectal cancer cells[20–22], suggesting that our data are consistent with the phenotype of METTL3 deficiency in terms of proliferation. These findings suggest that the suppression of colorectal cancer cell proliferation upon YTHDC1 knockdown is partially dependent on m^6A binding. To clarify the mechanism underlying the reduced cell proliferation caused by YTHDC1 deficiency, we first hypothesized that the cells underwent apoptosis. We conducted flow cytometry experiments with Annexin V staining on YTHDC1-deficient cells. The results revealed that YTHDC1 knockdown significantly enhanced cell apoptosis (Fig. 2f and Supplementary Fig. 1b).

To validate our in vitro findings, we subcutaneously injected YTHDC1-knockdown colorectal cancer cells into immunodeficient mice. Our results showed that the knockdown of YTHDC1 significantly impeded the growth of subcutaneous tumors (Fig. 2g–i). In summary, our in vitro and in vivo experimental results demonstrated that YTHDC1 plays a critical role in facilitating the proliferation of colorectal cancer cells, and knocking down YTHDC1 promotes apoptosis in these cells.

Knocking down YTHDC1 leads to the downregulation of RAD51 expression at the protein level through the ubiquitin-proteasome pathway

We explored the mechanisms by which the deletion of YTHDC1 inhibits the proliferation of CRC cells and induces cell apoptosis through an in-depth investigation of DNA repair processes. Recent studies have shown that the deficiency of either METTL3 or YTHDC1 can affect the recruitment of RAD51 to double-strand break (DSB) sites[10]. After knocking down YTHDC1 in HCT116 and SW480 cell lines, we observed a substantial reduction in the levels of the homologous recombination repair enzyme RAD51 (Fig. 3a). We further found that the depletion of RAD51 also suppressed cell proliferation and single-cell colony formation (Fig. 3b, c). This phenotype was consistent with that observed upon YTHDC1 knockdown, suggesting that RAD51 is one of the downstream targets of YTHDC1. Western blot experiments verified the knockdown efficiency of RAD51, and the results showed that the knockdown efficiency exceeded 90% (Fig. 3d). Meanwhile, we overexpressed RAD51 in the cells with YTHDC1 knockdown to perform the rescue experiments. The experimental results showed that overexpressing RAD51 could rescue the phenotype caused by YTHDC1 deficiency, elucidating that RAD51 is the downstream target through which YTHDC1 exerts its effect (Fig. 3e and Supplementary Fig. 2a).

Interestingly, RNA-sequencing results revealed no decrease in RAD51 expression at the transcriptional level following YTHDC1 knockdown (Fig. 3f). We hypothesized that the depletion of YTHDC1 might alter the post-translational modification levels of RAD51, with ubiquitination being the most probable modification. To validate this hypothesis, we used bortezomib to inhibit ubiquitin-mediated proteasomal degradation in YTHDC1-knockdown cells. The experimental results showed a reduction in RAD51 expression in the input sample but an increase in the ubiquitination level of RAD51 (Fig. 3g). Furthermore, we conducted protein degradation assays to determine whether YTHDC1 knockdown accelerated RAD51 degradation. We knocked down YTHDC1 and simultaneously added cycloheximide (CHX), a protein synthesis inhibitor, and then measured RAD51 protein expression at 0, 3, 6, 9, and 12 h. The results indicated that YTHDC1 knockdown slightly accelerated RAD51 degradation, but the effect was not statistically significant. This outcome may be closely associated with the degradation rate of RAD51 and the real-time expression level of YTHDC1 (Supplementary Fig. 2b). These findings suggest that the absence of YTHDC1 does not affect RAD51 transcription; rather, it promotes an increase in RAD51 ubiquitination levels.

YTHDC1 negatively regulates the expression of UBE3A and RAD51 is a substrate of UBE3A

Since YTHDC1 lacks ubiquitination activity, we hypothesize that an unknown E3 ubiquitin ligase may be negatively regulated by YTHDC1 and be responsible for the ubiquitination of RAD51. Through the analysis of RNA-sequencing data following YTHDC1 knockdown, we found that the expression of several ubiquitin-related enzymes was significantly upregulated, including the ubiquitin-protein ligase UBE3A (Fig. 4a). The Western blot results were consistent with the RNA-seq data (Fig. 4b). We tested the UBE3A and RAD51 expression through RT-qPCR after knocking down YTHDC1, the data indicated that YTHDC1 transcriptionally regulates UBE3A but not RAD51 (Supplementary Fig. 3a). By overexpressing YTHDC1, we found that the protein levels of UBE3A and RAD51 showed almost no change (Supplementary Fig. 3b). It is possible that because of the relatively high expression level of YTHDC1 in cells, the overexpressed protein is redundant. Overexpression does not yield results opposite to those of knockdown.

UBE3A is localized in both the nucleus and cytoplasm and has been reported to ubiquitinate RAD23A, thereby influencing global genome nucleotide excision repair (GG-NER)[23]. To further validate the relationship

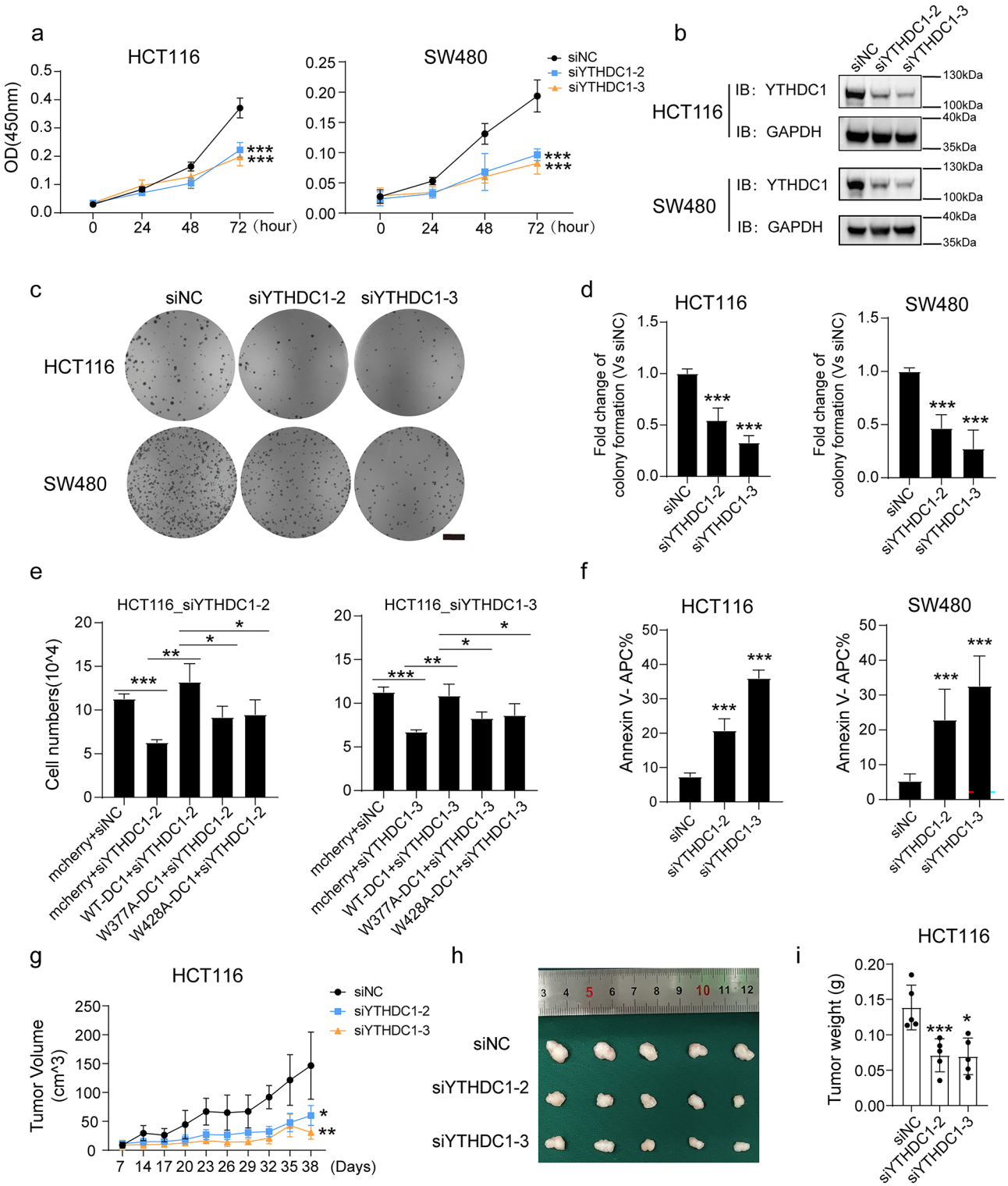

between UBE3A and RAD51, we performed co-immunoprecipitation (co-IP) experiments. We found that RAD51 interacts with UBE3A (Fig. 4c). In the ubiquitination assay, overexpression of UBE3A led to the ubiquitination of RAD51, showing a gradient-like change. As the expression level of UBE3A increased, the ubiquitination level of RAD51 also gradually increased (Fig. 4d). These findings indicate that UBE3A can ubiquitinate RAD51 and that RAD51 is one of the ubiquitination substrates of UBE3A.

We present a well-substantiated working model wherein YTHDC1, UBE3A, and RAD51 participate in crucial interactions at replication forks or DNA damage sites (Fig. 4e). When the expression of YTHDC1 is suppressed, the levels of UBE3A increase due to the regulatory influence of YTHDC1. This increase in UBE3A enhances the ubiquitination of RAD51, resulting in a significant decline in RAD51 protein expression. Such a reduction significantly impairs the progress of DNA replication and repair, ultimately triggering apoptosis in cancer cells.

◀**Fig. 2**. The deficiency of YTHDC1 suppresses the proliferate of colorectal cancer cells and increases apoptosis. (**a**) Proliferate curve of HCT116 and SW480 cells after knocking down YTHDC1. Data was analyzed by CCK8 with OD 450 nm. (**b**) Western blot analysis of YTHDC1 expression in HCT116 and SW480 cells after knocking down YTHDC1. (**c**) Colony formation analysis of HCT116 and SW480 cells after knocking down YTHDC1. The scale bar is 5 mm. (**d**) Quantification of colony numbers from Fig. 2c. (**e**) Effects of WT-YTHDC1, YTHDC1-W327A, or YTHDC1-W428A overexpression in YTHDC1-knocking down HCT116 cells. mCherry and siNC were the control for overexpressing plasmids and siRNAs. Cells were counted at day 2 after being transfected for 24 h. Synonymous mutations were introduced into the siRNA-targeting sequences of these plasmids to ensure the overexpression of exogenous genes. (**f**) Quantification of annexin V-APC positive cell percentage in Flow cytometry analysis after knocking down YTHDC1. (**g**) Growth curve of xenograft tumors from HCT116 cells. $n = 5$. (**h**) Xenograft tumors from HCT116 cells. (**i**) Quantification of tumor weight from Fig. 2F. $n = 5$. Data are presented as the mean ± SD of three independent experiments (**a**,**d**,**e**,**f**). $^{*}p < 0.05$, $^{**}p < 0.01$, $^{***}p < 0.001$; *NS* no significance; two-tailed Student's *t* test.

This model underscores the delicate equilibrium within cellular processes and the potential consequences of disturbing this balance.

Discussion

In this study, we demonstrated that YTHDC1 acts as a tumor-promoting factor in colorectal cancer. The molecular mechanism we elucidated reveals that the deletion of YTHDC1 leads to the upregulation of the E3 ubiquitin-protein ligase UBE3A. This upregulation, in turn, promotes the ubiquitination of the homologous recombination repair enzyme RAD51, ultimately inducing apoptosis in colorectal cancer cells.

One previous study has shown that METTL3 can significantly affect the transcription of nascent RNA at DNA damage sites[19]. Another publication reported that the depletion of METTL3 and YTHDC1 notably impacts the recruitment of RAD51 to DNA damage sites, ultimately affecting the efficacy of DNA repair[10]. These findings suggest that m^6A modification and YTHDC1 are intricately involved in the DNA damage repair process. Although our study was not conducted under DNA damage inducing conditions, we investigated the molecular level regulation of RAD51 by YTHDC1. Specifically, we discovered that YTHDC1 could stabilize the expression of the RAD51 protein by modulating UBE3A expression, thereby reducing excessive ubiquitination and inhibits apoptosis in colorectal cancer cells. Recent research has shown that YTHDC1 recognizes m^6A modifications and recruits histone-modifying enzymes to target gene loci, leading to target gene silencing[5,24]. Alternatively, it can accelerate RNA degradation, thereby enhancing chromatin accessibility and promoting transcription[25]. Therefore, in the model proposed in our study, m^6A may play a crucial role. Knocking down YTHDC1 might disrupt the genomic silencing state or impede RNA degradation, consequently promoting the expression of UBE3A.

In this study, we have identified a novel regulatory axis of YTHDC1-UBE3A-RAD51 in colorectal cancer. The negative regulation of UBE3A by YTHDC1 and its subsequent impact on RAD51 ubiquitination and cell apoptosis is a newly-discovered mechanism. This provides a fresh perspective on the role of YTHDC1 in tumor development, especially in the context of DNA repair-related processes. Secondly, our study reveals a new function of UBE3A in the ubiquitination of RAD51. Although UBE3A has been reported to be involved in other DNA repair-related pathways such as GG-NER[23], its role in regulating RAD51 ubiquitination in homologous recombination repair is a previously unreported discovery. This implies that UBE3A may be a significant and versatile E3 ubiquitin-protein ligase in DNA damage repair, not restricted to a specific repair pathway. This expands our understanding of the functions of UBE3A in the DNA damage response network.

The findings of our study hold significant potential for colorectal cancer treatment. Given that high expression of YTHDC1 is associated with poor prognosis and promotes tumor cell proliferation, targeting YTHDC1 could be a promising therapeutic strategy. Inhibiting YTHDC1 expression might lead to the upregulation of UBE3A, which in turn increases the ubiquitination and degradation of RAD51. Studies have demonstrated that the expression level of RAD51 is substantially higher in numerous cancers, including colorectal cancer, compared to normal tissues[26]. Elevated RAD51 levels can render tumor cells hyper-recombinogenic, contributing to resistance to radiotherapy and chemotherapy[27]. Our new finding shows that YTHDC1 knockdown disrupts the DNA repair ability of tumor cells, making them more sensitive to DNA-damaging agents such as chemotherapy drugs and radiotherapy. For example, in combination with traditional chemotherapeutic drugs, targeting YTHDC1 could enhance the efficacy of these drugs by reducing the repair capacity of cancer cells. Moreover, since UBE3A is a key factor in this regulatory pathway, modulating its activity could also be a potential therapeutic approach. If we can develop drugs that can specifically enhance the activity of UBE3A or promote its interaction with RAD51, it may also effectively inhibit the growth of colorectal cancer cells. Overall, our study provides new molecular targets and theoretical basis for the development of more effective colorectal cancer treatment methods.

Materials and methods

Cells and cell culture

Colorectal cancer cell lines HCT116 and SW480 were purchased from iCell company (Shanghai, China). HCT116 and SW480 were cultured in DMEM (Sigma-Aldrich,) supplemented with 10% fetal bovine serum (ExCell bio, FSP500), 1% nonessential amino acids (Gbico, 11140050), 1% Gluta-MAX (Gbico, 35050061), and 1% penicillin/streptomycin (Gbico, 15140122), at 37 °C with 5% CO_2.

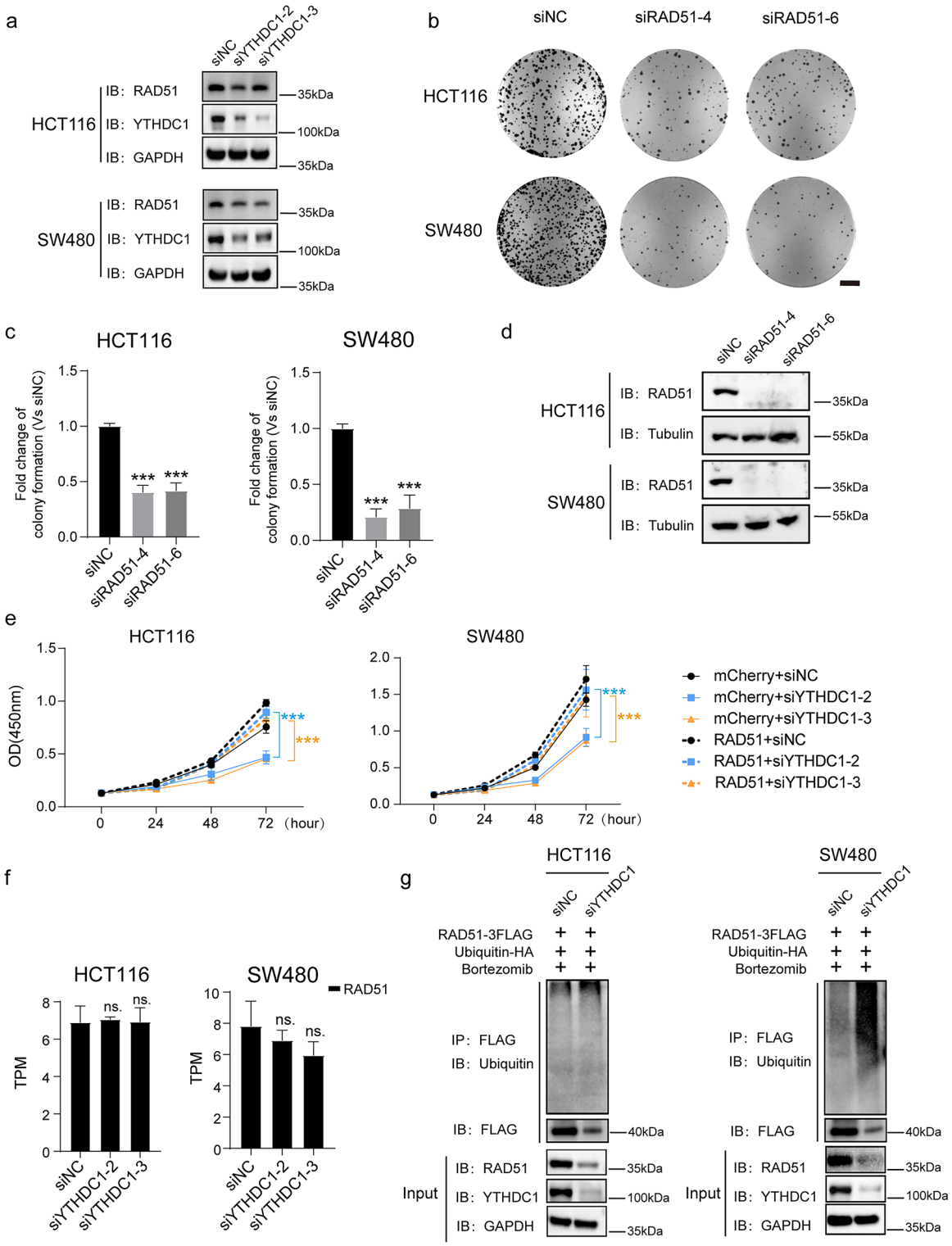

Fig. 3. Knocking down YTHDC1 leads to the downregulation of RAD51 expression at the protein level through the ubiquitin-proteasome pathway. (**a**) Western blot analysis of RAD51 expression in HCT116 and SW480 cells after knocking down YTHDC1. (**b**) Colony formation analysis of HCT116 and SW480 cells after knocking down YTHDC1. The scale bar is 5 mm. (**c**) Quantification of colony numbers from Fig. 2b. (**d**) Western blot analysis of RAD51 expression in HCT116 and SW480 cells after knocking down RAD51. (**e**) Effects of RAD51 overexpression in YTHDC1-knocking down HCT116 and SW480 cells. Data was analyzed by CCK8 with OD 450 nm. (**f**) The transcriptional expression of RAD51 from the RNA-seq dataset of HCT116 and SW480 cells after knocking down YTHDC1. (**g**) Control and YTHDC1-siRNA HCT116/SW480 cells transfected with ubiquitin-HA and RAD51-3FLAG were treated with bortezomib for 12 h before harvest. Data are presented as the mean ± SD of three independent experiments. $^{*}p < 0.05$, $^{**}p < 0.01$, $^{***}p < 0.001$; *NS* no significance; two-tailed Student's *t* test.

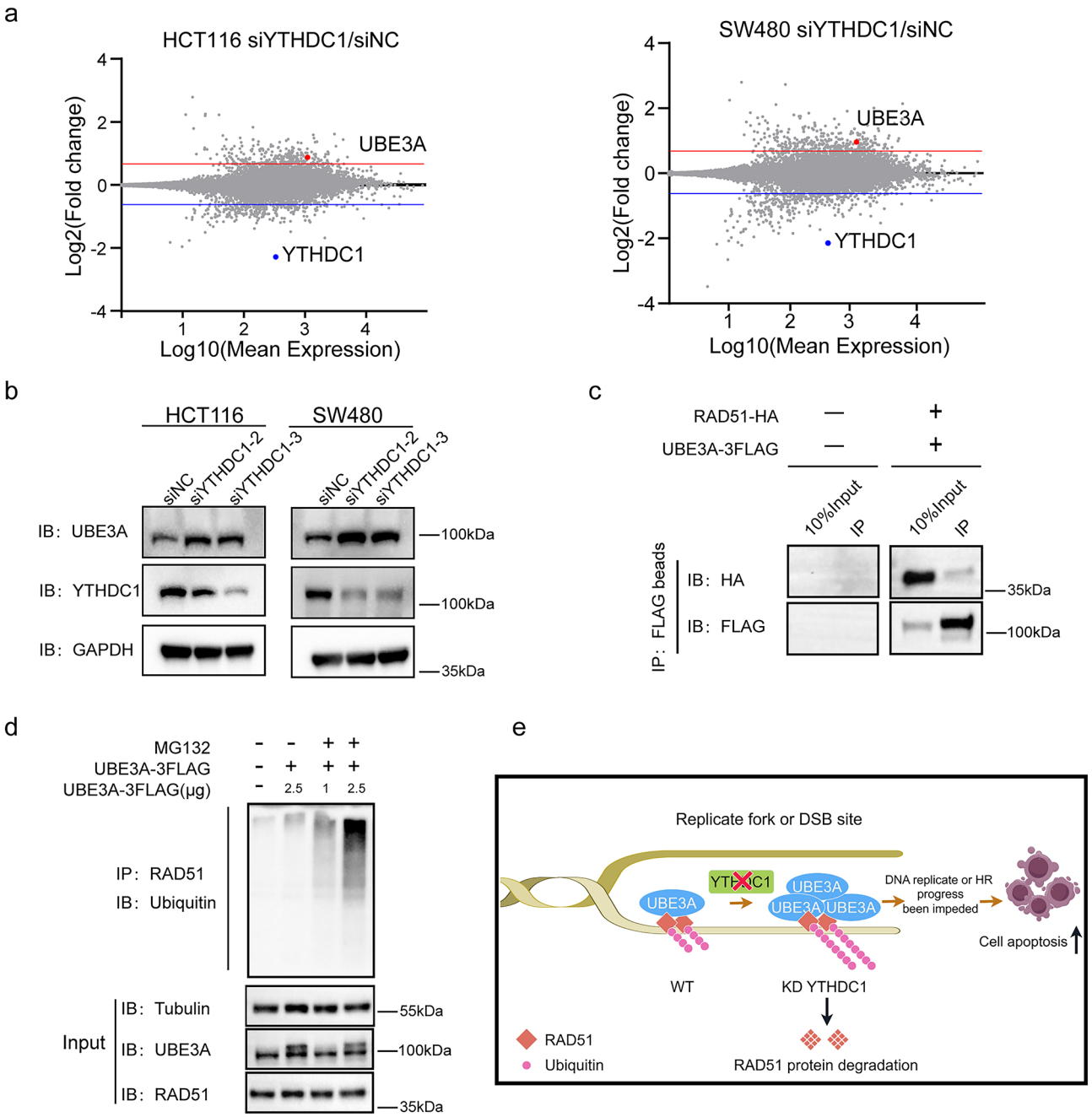

Fig. 4. YTHDC1 negatively regulates the expression of UBE3A and RAD51 is a substrate of UBE3A. (**a**) Volcano plots of genes after knocking down YTHDC1 in HCT116 and SW480 cell lines. Each dot represents a gene. Genes above the red line represented the expression were more than1.5 fold change compared to the control. Genes under the blue line represented the expression were less than 1.5 fold change compared to the control. (**b**) Western blot analysis of UBE3A upon knocking down YTHDC1 in HCT116 and SW480. (**c**) The interaction between RAD51 and UBE3A was detected by the co-IP experiment. (**d**) Detecting the ubiquitination level of RAD51 with gradient overexpression of UBE3A. (**e**) The hypothetical model of YTHDC1 regulates the ubiquitination level of RAD51 and induces apoptosis in colorectal cancer cells by negatively regulating the expression of UBE3A.

Cell transfection

Transfection of siRNAs was performed using Lipofectamine RNAiMAX transfection reagent (Thermo Fisher, 13778150). YTHDC1-siRNAs were designed and synthesized by Ribo-Bio (Guangzhou, China). RAD51-siRNAs were designed and synthesized by IGE Biotechnology (Guangzhou, China). The target sequence for siYTHDC1-2 is 5′-GGGAAATGATTATGACACT-3′, siYTHDC1-3 is 5′-GTATCAGGTCATTCATAAA-3′, siRAD51-4 is 5′-GCAGTGATGTCCTGGATAA-3′, and siRAD51-6 is 5′-CCAACGATGTGAAGAAATT-3′.

siNC (si control, siN0000001-1-5 siR NC #1) was purchased from RiboBio (Guangzhou, China). Plasmids were transfected by Lipo8000(Beyotime, C0533).

Plasmids construction

Human *YTHDC1*, *YTHDC1*-W377A, *YTHDC1*-W428A, *RAD51*, and mCherry were generated and cloned into the pRlenti-3Flag vector. Human *RAD51* was generated and cloned into the pRlenti-HA vector. pLV-CMV-UBE3A-3FLAG and pRK-HA-Ubiquitin were purchased from DINGKE Biotechnology (Shenzhen, China).

Cell viability assay

Cell viability was detected using a CCK8 kit (Yeason, 40203ES76). For proliferation assay, 4000 cells per well were added into 96-well plates in 100 µL culture medium. CCK8 was added into each well mixed with culture medium and incubated at 37 °C for 90 min. The absorbance at 450 nm was measured with a microplate reader (Biotek, SynergyH1) at different time points.

Colony formation assay

1500 cells per well were seeded into 6-well plates in 2 mL DMEM medium with 10% FBS. After 12–14 days, most colonies were visible. Cells were washed twice with PBS and fixed with 4% paraformaldehyde for 10 min. Then cells were stained with crystal violet at room temperature for 30 min. Colonies were photographed and counted with ImageJ software.

Apoptosis assay

Apoptosis assay was detected with APC Annexin V Apoptosis Detection Kit (Biolegend, 640932). 300,000 cells were harvested and washed twice with cold BioLegend's Cell Staining Buffer. Cells were collected after centrifuging at 1000 × g for 5 min. 100 µL Annexin V binding buffer was added to resuspend the cell sediment. 5 µL APC Annexin V was added and incubated with cells for 15 min at room temperature in the dark. Finally, each sample was mixed with 400 µL of Annexin V Binding Buffer and analyzed by flow cytometry with CytoFLEX LX (Beckman Coulter, USA).

In vivo animal study

Female NGS mice (5–6 weeks of age, 18–20 g) were purchased from Cyagen (Suzhou, China). HCT116 cells were resuspended in PBS at 3.5×10^6 cells/100 µL. 100 µL cell suspension was injected into one side of the subcutaneous axilla of the mice. The width and length of tumors were measured with a vernier caliper at designated time points. Cervical dislocation method was used to euthanize mice. The tumor volume was evaluated by the formula: $V = 1/2 \times \text{width}^2 \times \text{length}$. All experimental protocols were approved by the Institutional Review Board (or Ethics Committee) of Shenzhen Peking University-the Hong Kong University of Science and Technology (PKU-HKUST) Medical Center (protocol code 2022-047 and date of approval: 23 February 2022). All methods were performed in accordance with relevant guidelines and regulations. All methods are reported in accordance with ARRIVE guidelines.

Western blot

Cells were lysed by RIPA buffer with 1% PMSF and 1% Cocktail on ice for 30 min, and centrifuged with 13,500 × g at 4 °C for 15 min. The protein concentration was analyzed by a BCA assay kit (Beyotime, P0010S). Equal protein lysates were analyzed using 10% SDS-PAGE gels and transferred into the PVDF membrane (Millipore, USA). 5% milk in TBS buffer containing 0.1% Tween20 was used to block the membrane for 1 h at room temperature. After incubation with a primary antibody at 4 °C overnight, the membrane was hybridized with the secondary antibody at room temperature for 1 h. The protein visualization was achieved by the ECL Detection Reagent (Yeason, 36208ES60). The primary antibodies are as follows: YTHDC1 (Abcam, ab122340), GAPDH (Proteintech, 60004-1-Ig), Tubulin (Proteintech, 10094-1-AP), RAD51 (Abcam, 133534), Ubiquitin (CST, P4D1), HA (CST, 3724 S), FLAG (CST, 14793), UBE3A (Abcam, 126765).

RNA extraction and RNA sequencing

RNA was extracted from the cells according to the instructions of Total RNA Kit I (Omega, R6834). RNA-seq library was constructed as the instruction of VAHTS Universal V8 RNA-seq Library Prep Kit for Illumina (Vazyme, NR605-02). Libraries were single-end reads with a 75 bp read length or paired-end reads with a 150 bp read length. For RNA-seq, our samples were derived from the cell samples of siYTHDC1 in HCT116 and SW480. For each of the two cell lines, there were siNC (control) and two siRNAs for knocking down YTHDC1, with two replicates for each group. In total, there were 12 samples.

RNA-seq data analysis

The reference transcriptome index was produced with RSEM[28] using the reference genome hg38. The reads were mapped to the reference transcriptome using RSEM and bowtie 2 (with options 'rsem-calculate-expression -p 12–bowtie2–no-bamout')[29] and normalized using EDASeq[30]. We chose the Trans per Million (TPM) value to normalize and evaluate gene expression levels. RNA-seq data were expressed as GC-normalized tag counts for DESeq2 to analyze differential gene expression[31]. Genes were considered as differentially expressed if gene expression was more than 1.5-fold change and $p < 0.05$. Data analysis and visualization were performed by package in R.

Co-immunoprecipitation (co-IP)

Cells were lysed by lysis buffer (50 mM pH 7.5 Tris–HCl, 150 mM NaCl, 2 mM EDTA, 1% NP40) with 1% PMSF and 1% cocktail. Samples were sonicated for 5 cycles at 4 °C (low level, 30 s off, 30 s on) with the ultrasonic machine (Diagenode, Bioruptor Plus). Cells were centrifuged at 13,000 rpm 4 °C for 15 min. The supernatant was collected and divided into 3 tubes (20% Input, 40% IgG, and 40% IP). 2 μg Antibodies and 50 μL Protein A & G magnetic beads were added into the IgG or IP tubes simultaneously and incubated with the cells at 4 °C overnight. Samples were washed five times with wash buffer (same as lysis buffer). With the help of DynaMag™-2 Magnet (Invitrogen, USA), beads were collected after washing thoroughly. Beads were resuspended with RIPA lysis (concluded with 5× loading buffer, 1%PMSF, and 1% cocktail) and boiled to make proteins get off from the magnetic beads. Proper volume RIPA lysis buffer was added to the Input sample to make the same volume as IgG/IP samples. Protein samples were analyzed using the western blot described before. The IP antibodies are as follows: Flag (Sigma, F1804), RAD51 (Abcam, 133534), Flag beads (HUABIO, HAK21011).

Tissue microarray and immunohistochemistry (IHC)

The tissue microarray (Cat. D160Co01S) was purchased from Bioaitech Co., Ltd (Xi'an, China), which contains 80 cases of colon cancer tissues and their matched adjacent tissues. The study using the tissue microarray was approved by the Life Sciences Ethics Committee of Changsha Yaxiang Biotechnology Co., LTD. The Ethics report is available online at yxswll.ccrl.cn. The query code is YZHQHER6RA9Y1M. The informed consent was obtained from all patients. Immunohistochemistry (IHC) was conducted to evaluate YTHDC1 in colonic adenocarcinoma. Antibodies used was YTHDC1(Abcam, ab122340). Slides were baked at 60 °C for 30 min for conventional dewaxing and hydration. After heating 0.01% sodium citrate buffer (pH 6.0) in a microwave oven until it boils, the tissue chip was placed in the oven for antigen repair. Then the power was cut off, and the repair of the antigen was repeated twice every 5–10 min. The tissue chip was cooled to room temperature and washed with PBS for 5 min × 3 times. Endogenous peroxidase was blocked with 3% H_2O_2-methanol at room temperature for 30 min and the tissue chip was washed with PBS for 5 min × 3 times. Normal non-immune animal serum was added to the chip dropwise and incubated at room temperature for 10 min. After discarding the serum, the antibody anti-YTHDC1(Abcam, ab122340) was added to the tissue chip and incubated at 4 °C overnight. The tissue chip was washed with 0.1% Tween-20 PBS for 5 min × 3 times. Enzyme-linked polymer secondary antibody was added and incubated at 37 °C in a wet box for 30 min. The tissue chip was washed with 0.1% Tween-20 PBS for 5 min × 3 times. After the DAB reagent colored the tissue chip for 5 min, distilled water was used to wash the tissue chip to terminate the coloring. The tissue chip was re-sustained with hematoxylin and fully washed with water to return to blue, and then dehydrated to become transparent and sealed with neutral gum successively. We used a scoring method based on percent positivity[32–34]. YTHDC1 was scored as the number of positive tumor cells over total tumor cells (0-100%). It can be classified as follows: (−) means that the positive cells are less than 10%, (+) means that the number of positive cells is between 10 and 25%, (++) means that the number of positive cells is between 26 and 49%, and (+++) means that the number of positive cells is more than 50%. At least 5–10 high-power fields (HPF) are randomly observed, and the average value is taken.

Data availability

Sequence data that support the findings of this study have been deposited in the Gene Expression Omnibus of NCBI with the primary accession code GSE245860. https://www.ncbi.nlm.nih.gov/geo/query/acc.cgi?acc=GSE245860.

Received: 2 December 2024; Accepted: 3 March 2025
Published online: 14 March 2025

References

1. Yang, Y., Hsu, P. J., Chen, Y. S. & Yang, Y. G. Dynamic transcriptomic m(6)A decoration: writers, erasers, readers and functions in RNA metabolism. *Cell. Res.* **28**, 616–624. https://doi.org/10.1038/s41422-018-0040-8 (2018).
2. Jiang, X. et al. The role of m6A modification in the biological functions and diseases. *Signal. Transduct. Target. Ther.* **6**, 74. https://doi.org/10.1038/s41392-020-00450-x (2021).
3. Meyer, K. D. & Jaffrey, S. R. Rethinking m(6)A readers, writers, and erasers. *Annu. Rev. Cell. Dev. Biol.* **33**, 319–342. https://doi.org/10.1146/annurev-cellbio-100616-060758 (2017).
4. Xu, C. et al. Structural basis for selective binding of m6A RNA by the YTHDC1 YTH domain. *Nat. Chem. Biol.* **10**, 927–929. https://doi.org/10.1038/nchembio.1654 (2014).
5. Liu, J. et al. The RNA m6A reader YTHDC1 silences retrotransposons and guards ES cell identity. *Nature* **591**, 322–326. https://doi.org/10.1038/s41586-021-03313-9 (2021).
6. Li, Y. et al. N(6)-Methyladenosine co-transcriptionally directs the demethylation of histone H3K9me2. *Nat. Genet.* **52**, 870–877. https://doi.org/10.1038/s41588-020-0677-3 (2020).
7. Xiao, W. et al. Nuclear m(6)A reader YTHDC1 regulates mRNA splicing. *Mol. Cell.* **61**, 507–519. https://doi.org/10.1016/j.molcel.2016.01.012 (2016).
8. Roundtree, I. A. et al. YTHDC1 mediates nuclear export of N(6)-methyladenosine methylated mRNAs. *Elife* **6**. https://doi.org/10.7554/eLife.31311 (2017).
9. Sheng, Y. et al. A critical role of nuclear m6A reader YTHDC1 in leukemogenesis by regulating MCM complex-mediated DNA replication. *Blood* **138**, 2838–2852. https://doi.org/10.1182/blood.2021011707 (2021).
10. Zhang, C. et al. METTL3 and N6-methyladenosine promote homologous recombination-mediated repair of DSBs by modulating DNA-RNA hybrid accumulation. *Mol. Cell* 79, 425–442 e427. https://doi.org/10.1016/j.molcel.2020.06.017 (2020).
11. Du, Y. et al. METTL3 promotes homologous recombination repair and modulates chemotherapeutic response in breast cancer by regulating the EGF/RAD51 axis. *eLife* **11** https://doi.org/10.7554/eLife.75231 (2022).
12. Liu, S. P. et al. The roles and mechanisms of YTH domain-containing proteins in cancer development and progression. *Am. J. Cancer Res.* **10**, 1068–1084 (2020).

13. Zhang, Z. L. et al. YTHDC1 mitigates ischemic stroke by promoting Akt phosphorylation through destabilizing PTEN mRNA. *Cell. Death Dis.* **11**, 977. https://doi.org/10.1038/s41419-020-03186-2 (2020).
14. Zeng, W. et al. m6A-modified circFNDC3B inhibits colorectal cancer stemness and metastasis via RNF41-dependent ASB6 degradation. *Cell. Death Dis.* **13** https://doi.org/10.1038/s41419-022-05451-y (2022).
15. Chen, R. X. et al. N6-methyladenosine modification of circNSUN2 facilitates cytoplasmic export and stabilizes HMGA2 to promote colorectal liver metastasis. *Nat. Commun.* **10**. https://doi.org/10.1038/s41467-019-12651-2 (2019).
16. Bonilla, B., Hengel, S. R., Grundy, M. K. & Bernstein, K. A. RAD51 gene family structure and function. *Annu. Rev. Genet.* **54**, 25–46. https://doi.org/10.1146/annurev-genet-021920-092410 (2020).
17. Bhat, K. P. & Cortez, D. R. P. A. RAD51: fork reversal, fork protection, and genome stability. *Nat. Struct. Mol. Biol.* **25**, 446–453. https://doi.org/10.1038/s41594-018-0075-z (2018).
18. Yu, D. et al. Human MettL3-MettL14 RNA adenine methyltransferase complex is active on double-stranded DNA containing lesions. *Nucleic Acids Res.* **49**, 11629–11642. https://doi.org/10.1093/nar/gkab460 (2021).
19. Xiang, Y. et al. RNA m(6)A methylation regulates the ultraviolet-induced DNA damage response. *Nature* **543**, 573–576. https://doi.org/10.1038/nature21671 (2017).
20. Zhou, D. et al. METTL3/YTHDF2 m6A axis accelerates colorectal carcinogenesis through epigenetically suppressing YPEL5. *Mol. Oncol.* **15**, 2172–2184. https://doi.org/10.1002/1878-0261.12898 (2021).
21. Li, T. et al. METTL3 facilitates tumor progression via an m6A-IGF2BP2-dependent mechanism in colorectal carcinoma. *Mol. Cancer*. **18**. https://doi.org/10.1186/s12943-019-1038-7 (2019).
22. He, R. Z. et al. Stabilization of UCA1 by N6-methyladenosine RNA methylation modification promotes colorectal cancer progression. *Cancer Cell. Int.* **21**. https://doi.org/10.1186/s12935-021-02288-x (2021).
23. Kumar, S., Talis, A. L. & Howley, P. M. Identification of HHR23A as a substrate for E6-associated protein-mediated ubiquitination. *J. Biol. Chem.* **274**, 18785–18792. https://doi.org/10.1074/jbc.274.26.18785 (1999).
24. Xu, W. et al. METTL3 regulates heterochromatin in mouse embryonic stem cells. *Nature* **591**, 317–321. https://doi.org/10.1038/s41586-021-03210-1 (2021).
25. Liu, J. et al. N (6)-methyladenosine of chromosome-associated regulatory RNA regulates chromatin state and transcription. *Science (New York N Y)*. **367**, 580–586. https://doi.org/10.1126/science.aay6018 (2020).
26. Laurini, E. et al. Role of Rad51 and DNA repair in cancer: A molecular perspective. *Pharmacol. Ther.* **208**. https://doi.org/10.1016/j.pharmthera.2020.107492 (2020).
27. Tennstedt, P. et al. RAD51 overexpression is a negative prognostic marker for colorectal adenocarcinoma. *Int. J. Cancer* **132**, 2118–2126. https://doi.org/10.1002/ijc.27907 (2012).
28. Li, B. & Dewey, C. N. RSEM: accurate transcript quantification from RNA-Seq data with or without a reference genome. *BMC Bioinform.* **12**, 323. https://doi.org/10.1186/1471-2105-12-323 (2011).
29. Langmead, B. & Salzberg, S. L. Fast gapped-read alignment with bowtie 2. *Nat. Methods* **9**, 357–359. https://doi.org/10.1038/nmeth.1923 (2012).
30. Risso, D., Schwartz, K., Sherlock, G. & Dudoit, S. GC-content normalization for RNA-Seq data. *BMC Bioinform.* **12**, 480. https://doi.org/10.1186/1471-2105-12-480 (2011).
31. Love, M. I., Huber, W. & Anders, S. Moderated Estimation of fold change and dispersion for RNA-seq data with DESeq2. *Genome Biol.* **15**, 550. https://doi.org/10.1186/s13059-014-0550-8 (2014).
32. Zlobec, I., Terracciano, L., Jass, J. R. & Lugli, A. Value of staining intensity in the interpretation of immunohistochemistry for tumor markers in colorectal cancer. *Virchows Arch.* **451**, 763–769. https://doi.org/10.1007/s00428-007-0466-8 (2007).
33. Lugli, A. et al. Role of the mitogen-activated protein kinase and phosphoinositide 3-kinase/AKT pathways downstream molecules, phosphorylated extracellular signal-regulated kinase, and phosphorylated AKT in colorectal cancer—A tissue microarray-based approach. *Hum. Pathol.* **37**, 1022–1031. https://doi.org/10.1016/j.humpath.2006.03.002 (2006).
34. Lugli, A. et al. Overexpression of the receptor for hyaluronic acid mediated motility is an independent adverse prognostic factor in colorectal cancer. *Mod. Pathol.* **19**, 1302–1309. https://doi.org/10.1038/modpathol.3800648 (2006).

Author contributions

Conceptualization: M.G.; methodology: M.G., Y.W., L.Z., Y.Z., H.L.; validation: M.G., Y.W., L.Z., Y.Z., H.L.; formal analysis: M.G.; investigation: M.G., Y.W.; writing—original draft preparation: M.G.; visualization: M.G.; writing—review and editing: M.G., W.Z., Y.C.; supervision: W.Z., S.W., Y.C.; funding acquisition: M.G., W.Z., S.W., Y.C. All authors have read and agreed to the published version of the manuscript.

Funding

This research was funded by the funds of Guangdong Basic and Applied Basic Research Foundation, grant number 2019B030302012, the National Key R&D Program of China, grant number 2021YFC2501001, Shenzhen Medical Research Funds, grant number C2303002, the National Natural Science Foundation of China, grant number 82341024, U21A20372, 82172930 and 82203286, the China National Postdoctoral Program for Innovative Talents, grant number BX20220214, Major Program of Shenzhen Bay Laboratory, grant number S201101004, Shenzhen "San-Ming" Project of Medicine, grant number SZSM202311014 and SZSM202211036, Shenzhen Science and Technology Innovation Commission Project, grant number ZDSYS20190902092855097 and KCXFZ20200201101050887.

Declarations

Competing interests

The authors declare no competing interests.

Consent for publication

Each author approved the manuscript before submission for publication.

Additional information

Supplementary Information The online version contains supplementary material available at https://doi.org/10.1038/s41598-025-92925-6.

Correspondence and requests for materials should be addressed to S.W. or Y.C.